

Experimental Investigation to Study Flow Characteristics over a Naca0018 Aerofoil and an Automobile Dome-A Comparative Study

M. Sri Rama Murthy¹, A. V. S. S. K. S. Gupta²

¹Associate professor, Department of mechanical engineering, Sir C.R.R.College of Engineering, Eluru-534007, A.P, India, Mobile number: 091 09581958157.

²Professor Department of mechanical engineering, JNTUH College of engineering, Hyderabad – 72, A.P., India, Mobile number: 091 09849427331.

Abstract

Experiments are carried out to study static pressure distribution and drag variations over NACA0018 aerofoil and over an automobile dome. Static pressure coefficients are calculated along the chord length for different angles of attack for both the test models and the results are compared. Further, the relationship between coefficient of drag and Reynolds number has been arrived for different angles of incidence. It was found that coefficient of drag decreases as the Reynolds number increases and c_d is higher at higher angles of incidence for both the aerofoil and automobile dome.

Key words: Wind Tunnel; Angle of Attack (AOA); Pressure Coefficient; Drag coefficient; Reynolds number.

Notation

A	Projected area of aerofoil, m ²
C _d	drag coefficient
C _p	Pressure coefficient
F _d	drag force, N
L _c	Characteristic length, mm
LE	Leading Edge
P	Static pressure, mm of water
P _{amb}	ambient pressure, mm of water
q	Difference of manometer reading, cm
Re	Reynolds number based on velocity of air and characteristic length of aerofoil
TE	Trailing Edge
V	Velocity of air, m/s
Greek letters	
α	Angle of attack, degrees
ρ	Density of air, kg/m ³
μ	Dynamic viscosity of air, Ns/m ²
Subscripts	
d	drag
p	pressure
amb	ambient

I. Introduction

The study of Aerodynamics is an important aspect of automobile design. Drag is an important parameter for automobiles cruising at speeds of 80

kmph or greater, and thus the fine tuning of aerodynamics can lead to significance decrease in fuel consumption. Factors that affect aerodynamics are friction drag and pressure drag, where the former is associated with the interface of the vehicle and the air, and the latter is associated with the pressure gradients, wakes and eddies. In very simple terms, the flow over a vehicle's body is lower in pressure than that underneath due to the vehicle's shape and the longer path of the travel over the vehicle top, thereby producing an upward force to the vehicle. In light of these difficulties, automobile manufacturers have experimented with many shapes and conducted studies for better aerodynamic characteristics. Anderson, Jr, J.D. [1] has clearly given the fundamental aspects of fluid dynamics. He has mentioned the physics of continuity, momentum and energy equations in his book. Experimental investigation of aerodynamics of a car has been conducted by Desai M. et.al [2]. In this, measurement of pressures has been done over an exterior profile of car using two experimental approaches. Harris yang & Randy chang [3] have conducted experiments to explore the lift and drag effects of a rear wing mounted on a vehicle model. In this, they have noticed increase in drag associated with increased down force. Islam M.M. and Mamun M. [4] have conducted CFD simulations over a car body to analyze drag. In this, optimization of car geometry was studied to reduce the drag. Muyl.F. et.al [5] had developed a Hybrid method for aerodynamic shape optimization in automotive industry. Here, the optimization method couples a stochastic genetic algorithm and a deterministic BFGS hill-climbing method. Petrushov V.A. [6] has developed an improved method to determine the vehicle aerodynamic drag and rolling resistance. Singh S.N. et.al [7] had developed the momentum injection method to control the boundary layer separation using a rotating cylinder. In this, the coefficient of drag was reduced by 35 % approx. Strachan R. et.al [8] have conducted studies to compare CFD and experimental results of Ahmed reference model. The aim of the study was to investigate the ability of both the k-e and Reynolds stress viscous model to predict the alterations in the flow around the model when in

wall proximity in comparison with the isolated case. Time –averaged phenomenological investigation of a wake behind a bluff body has been conducted by Van Raemdonk G.M.R. and Van Tooren M.J.L [9]. In this; studies are conducted to know the change in drag, base pressures, the thickness of the boundary layers and the structure of the wake by varying fore body roughness on a bluff body. In the present paper, an attempt has been made to study flow characteristics over an aerofoil surface and an automobile dome and the results are compared. The objectives of the work are as follows.

- To calculate static pressure coefficients by measuring pressure distribution on the surfaces of both the test models.
- To arrive the relationship between the coefficient of pressure and the non-dimensional distance along the chord length and to compare the results for both the test models.
- To calculate drag coefficient by measuring drag force.
- To arrive the relationship between the coefficient of drag and Reynolds number for different angles of attack for both the models.

II. Materials and Methods

Experiments are carried out in a wind tunnel and the details are as follows :

Altech open circuit wind tunnel is designed for use in student Engineering laboratories and other industrial and Government research facilities. This Wind Tunnel can be used to study the pressure distribution and lift drag characteristics of airfoils, cylinder etc. Reynolds number up to 25, 00,000 can be achieved with this tunnel. The wind tunnel used for experimentation is shown in the fig1.

The wind tunnel is of suction type with an axial flow fan driven by a variable speed DC motor. It consists of an entrance section with a bell mouth inlet containing a flow straightener, screens and a straw honey comb. This section is followed by a 6.25:1 contraction section, the test section, a diffuser and the duct containing the axial flow fan. The whole unit is supported on steel frames. The complete wind tunnel except the test section is constructed of mild steel iron sheets for strength and rigidity. The test section is made of teak wood and has glass window for visual observation of flow phenomena. The control of the DC motor is by a rectifier controlled variable speed drive. The experiment has been carried out in subsonic wind tunnel with a test section 300 mm high 300mm wide and 800 mm long. The aerofoil and the automobile dome have been fixed along the width of the test section.

Pressure tapping is arranged at the 7 different locations on the surfaces of the aerofoil and automobile dome and connected to the manometer limbs to measure pressure variations. Measurement of free stream velocity is performed using a Pitot tube

and with a linkage mechanism transducer to determine drag force. A protractor is attached to the aerofoil & the automobile dome and is fitted in the side wall of the wind tunnel to measure the angle of rotation of the aerofoil & the automobile dome.

2.1 Aerofoil details

A test model of NACA0018 aerofoil has been selected for this study. The aerofoil is made of aluminum material with a chord of 16cm and a span of 25cm. The fig. 2 shows the details of aerofoil. Holes of 7 number of each 1mm diameter are drilled on the upper surface of the aerofoil. Flexible tubes are fixed at these 7 locations and connected to multitube manometer for measurement of static pressure distribution.

2.2 Automobile dome details

A second test model of an automobile dome has been selected for this study. The dome is made of plastic material with a projected chord length of 300 mm and a span of 150 mm. The fig. 3 gives the details of the automobile dome.

The measurements are taken for the following parameters

- Angle of attack (α) = 0° - 40°
- Reynolds number = 2.5×10^5 for the aerofoil and
- Reynolds number = 5×10^5 for the automobile dome

III. RESULTS AND DISCUSSIONS

3.1 Static pressure distribution

The static pressure distribution on the upper surface of a NACA0018 airfoil and on the surface of the automobile dome has been measured by using multi-tube manometer. From the results it is observed that pressure distribution varies with the non dimensional distance.

The pressure coefficient, C_p values are determined using the following relation.

$$C_p = (P_{amb} - P) / q \quad (1)$$

Where q = difference of manometer reading in cm.

Pressure coefficient values are determined along the chord length at 7 different locations for angles of attack i.e. $\alpha = 0^{\circ}, 10^{\circ}, 20^{\circ}, 30^{\circ}$ and 40° and arrived the relationship between coefficient of pressure and non-dimensional distance for both the cases i.e. aerofoil and automobile dome.

Reynolds number is calculated using the relation

$$R_e = V L_c / \nu \quad (2)$$

Figures 4, 5, 6, 7 and 8 show the variation of pressure coefficient with non-dimensional distance at

different angles of attack $\alpha = 0^\circ, 10^\circ, 20^\circ, 30^\circ$ and 40° .

From the figure 4, for an angle of attack 0° , it is observed that pressure coefficient decreases on the upper surface of the aerofoil up to some points of chord length and then slight increase in c_p takes place at very nearer to the trailing edge of the airfoil. This behavior is due to adverse pressure gradient at the trailing edge. The changes in c_p values are very marginal along the surface of the automobile dome. Also is observed that c_p values are higher for automobile dome when compared with the NACA 0018 Aerofoil and difference in values of c_p is marginal.

From the figure 5, for an angle of attack 10° , it is observed that the coefficient of pressure varies with the non dimensional distance for both the test models. The coefficient of pressure values are decreased on the upper surface of the aerofoil and on the surface of the automobile dome. The changes in c_p values are marginal along the upper surface of the aerofoil as well as on the surface of the automobile dome. Also it is observed that the coefficients of pressure values are higher for NACA 0018 Aerofoil when compared with the automobile dome. Almost all similar behavior was observed for the angles of attack $\alpha = 20^\circ, 30^\circ$ and 40° as shown in the figures 6, 7 and 8 respectively.

3.2 Drag variations

The drag coefficient values are determined using the following relations. The air flow velocity is determined from Pitot tube using the equation

$$v = 13\sqrt{q} \quad (3)$$

The coefficient of drag, C_d is determined using the following relation for both the test models at different velocities v and angles of attack α .

$$C_d = \frac{2F_d}{\rho AV^2} \quad (4)$$

Fig.9 shows the relationship between the coefficient of drag, C_d and Reynolds number for different angles of attack for the model NACA 0018 aerofoil. It is observed that the drag coefficient is larger at higher angles of attack and drag coefficient decreases as the Reynolds number increases. This behavior can be explained as follows. Since the boundary layer separation is not a factor at low Reynolds Number, the pressure drag is less. Whereas viscous drag increases considerably at the surface, simply because of the increased surface area over which the frictional stresses act. Thus total drag is actually increased by stream lining at low Reynolds number. Changes in the angles of attack alter the pressure distribution, particularly on the upper surface. As the angles of incidence increases, the main flow separates from the upper surface because

the shape downstream of the foil shoulder is such as to produce a severe rate of pressure rise leads to boundary layer separation and consequently to a larger pressure drag. Then total drag is increased greatly and lift suddenly decreases.

Fig.10 shows the drag variations with the Reynolds number at different angles of attack for the automobile dome. It is observed that the drag coefficient decreases as the Reynolds number increases and the coefficient of drag is higher as the angle of attack increases at the given Reynolds number. The reasons for this behavior are same as explained for the aerofoil.

IV. Conclusions

The static pressure distribution and drag variations over the surfaces of NACA 0018 aerofoil and an automobile dome were investigated experimentally. The angle of attack was varied in the range of $0^\circ \leq \alpha \leq 40^\circ$ at Reynolds number 2.5×10^5 for the aerofoil and at Reynolds number 5×10^5 . The following conclusions were drawn from the study.

From the static pressure distribution, it was concluded that pressure coefficient decreases on the upper surface of the aerofoil and slight increase in c_p value reported at very nearer to the TE of the aerofoil. The changes in c_p values are very marginal along the surface of the automobile dome and the c_p values are higher for automobile dome when compared with the aerofoil at 0° angle of attack. But the trend is reverse i.e. C_p values are lower for automobile dome when compared with the aerofoil for all other angles of attack i.e. $10^\circ, 20^\circ, 30^\circ$ and 40° .

From the drag studies, it was concluded that coefficient of drag, C_d decreases as the Reynolds number increases and the drag coefficient values are higher at the larger angles of attack for the given Reynolds number for both the models.

V. Acknowledgements

I express my deep gratitude and thanks to the management of Sir CRR College of engineering, Eluru for providing facilities and support to do my research work. But they are not involved in study design; in collection, analysis and interpretation of data; in the writing of the report; and in the decision to submit the article for publication.

References

- [1] Anderson Jr, J.D., Computational fluid dynamics: The Basics with Applications. Mc Graw-Hill, Inc, New York, 1995.
- [2] Desai M. et.al, a comparative assessment of two experimental methods for aerodynamic performance evaluation of a car, Journal of

scientific & Industrial research, vol.67, July 2008, pp 518-522.

- [3] Harris Yong & Randy Chang lift and drag effects of a rear wing on a passenger vehicle, Independent lab project, 1997.
- [4] Islam M.M. & Mamun M., computational drag analysis over a car body, Proc.of international conference on Marine Technology, 11-12 December 2010, Dhaka, Bangladesh, pp 155-158.
- [5] Muyl F. et.al, Hybrid method for aerodynamic shape optimization in automotive industry, computers & fluids, 33(2004) 849-858.
- [6] Petrushov VA, Improvements in vehicle aerodynamic drag and rolling resistance determination from coast-down tests, Proc Instn Mech Engrs Vol 212 Part D, 1998, pp 369-380.
- [7] Singh S.N. et.al, Effect of moving surface on the aerodynamic drag of road vehicles, Proc Instn Mech Engrs Vol 219 Part D: J.Automobile Engineering, 2005, pp 127-134.
- [8] Strachan R. et.al, Comparisions between CFD and experimental results for a simplified car model in wall proximity, Dept.of Aerospace, power and sensors, Cranfield University, LA.
- [9] Van Raemdonck G.M.R. & VanTooren M.I.L., Time-Averaged Phenomenological

investigation of a wake behind a bluff body, 6th International colloquium on: bluff bodies aerodynamics & applications, Milano, Italy, July, 20-24, 2008.

Figure captions

- Fig.1 : Experimental set up
- Fig 2: Aerofoil details
- Fig 3: Automobile dome
- Fig.4: Relationship between coefficient of pressure & non-dimensional distance at 0 degrees AOA
- Fig.5: Relationship between coefficient of pressure & non-dimensional distance at 10 degrees AOA
- Fig .6: Relationship between coefficient of pressure & non-dimensional distance at 20 degrees AOA
- Fig .7: Relationship between coefficient of pressure & non-dimensional distance at 30 degrees AOA
- Fig .8: Relationship between coefficient of pressure & non-dimensional distance at 40 degrees AOA
- Fig.9: Drag coefficient with Reynolds number for different angles of attack for NACA 0018 aerofoil
- Fig.10: Drag coefficient with Reynolds number for different angles of attack for an automobile dome

Figures

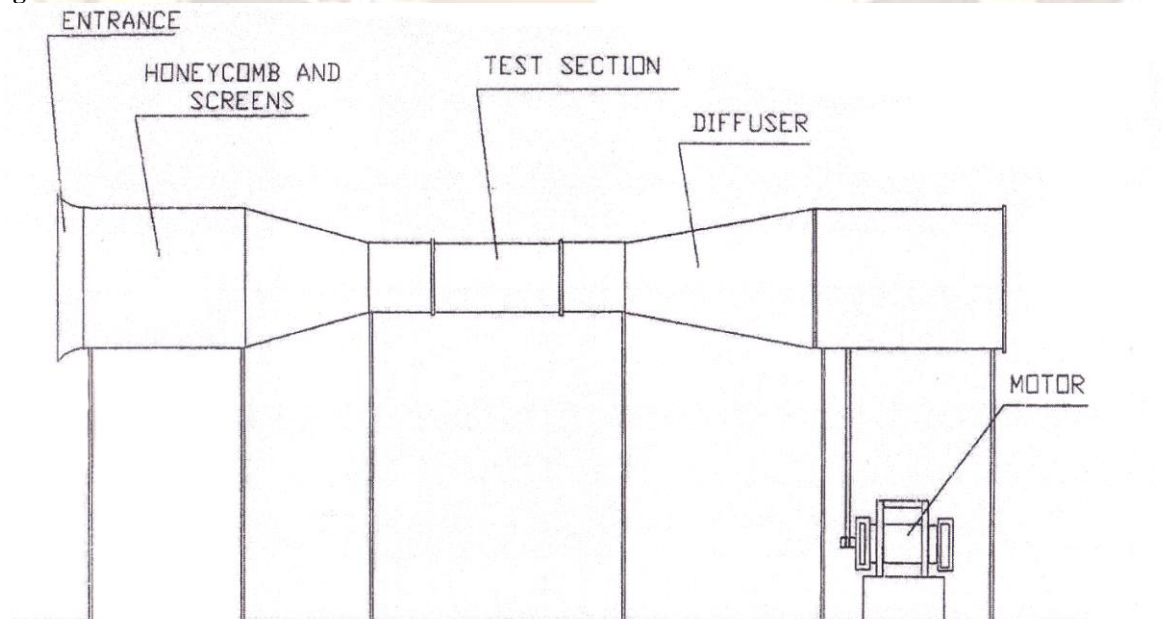


Fig.1

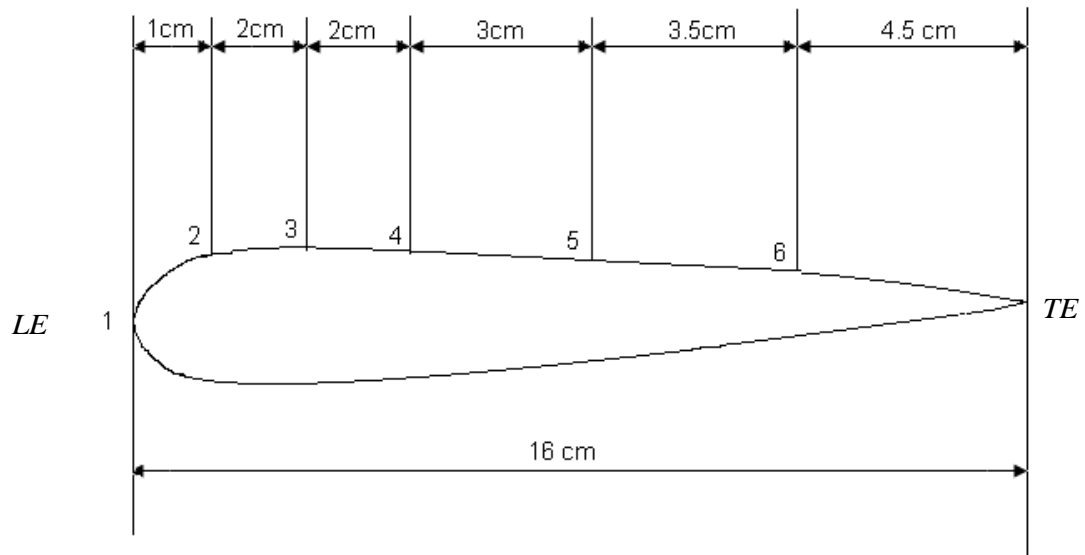


Fig.2



Fig.3

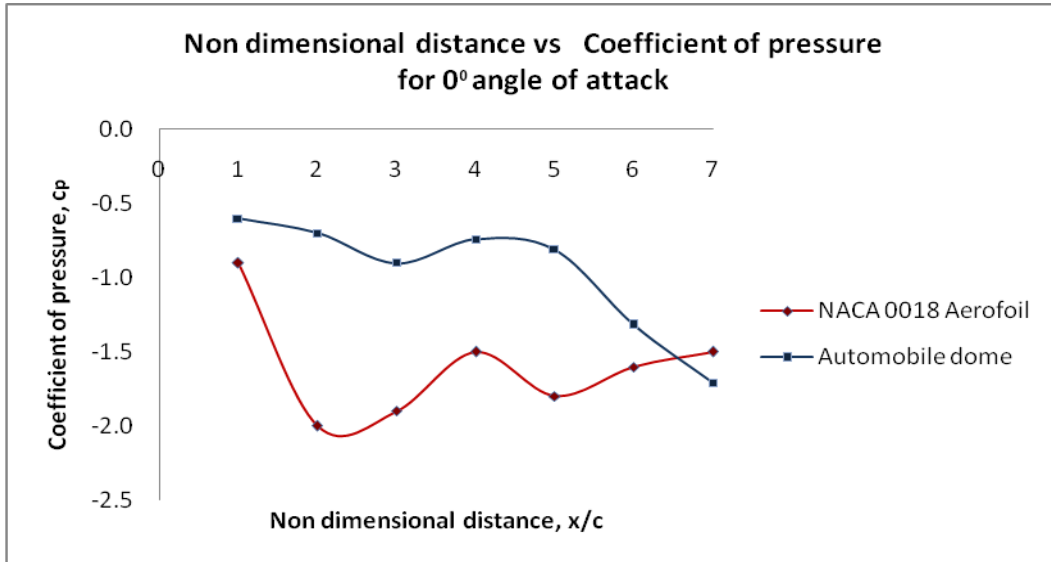


Fig.4

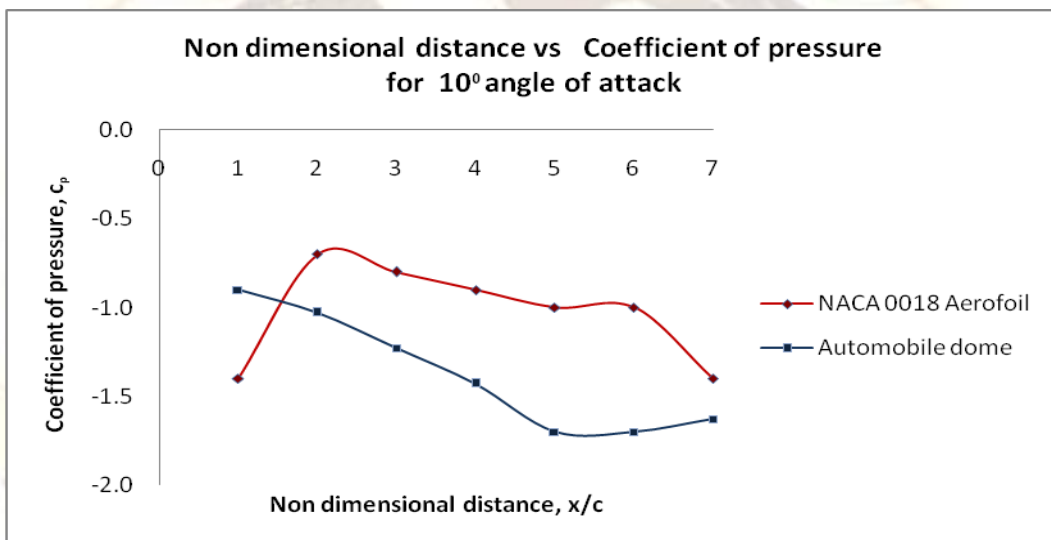


Fig.5

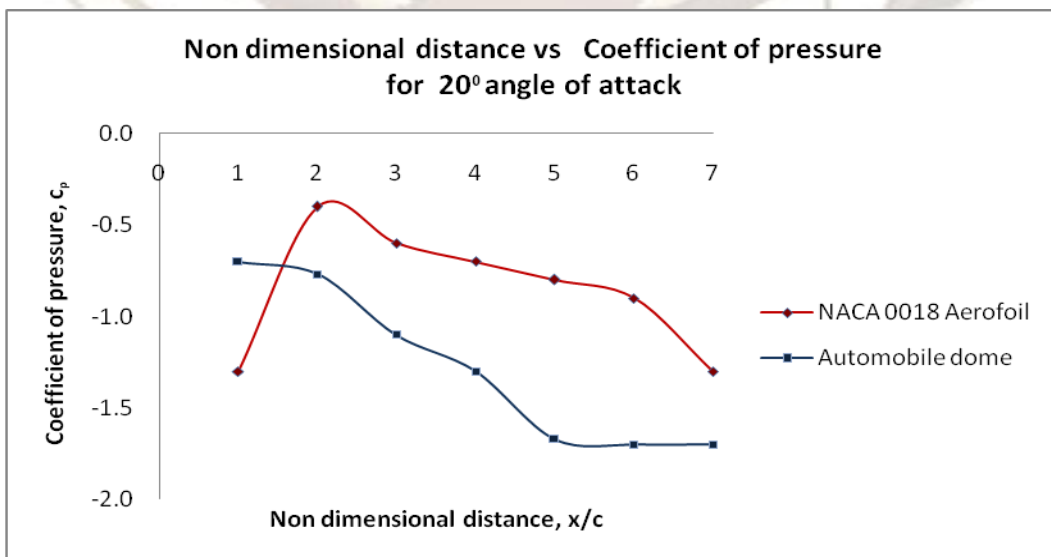


Fig.6

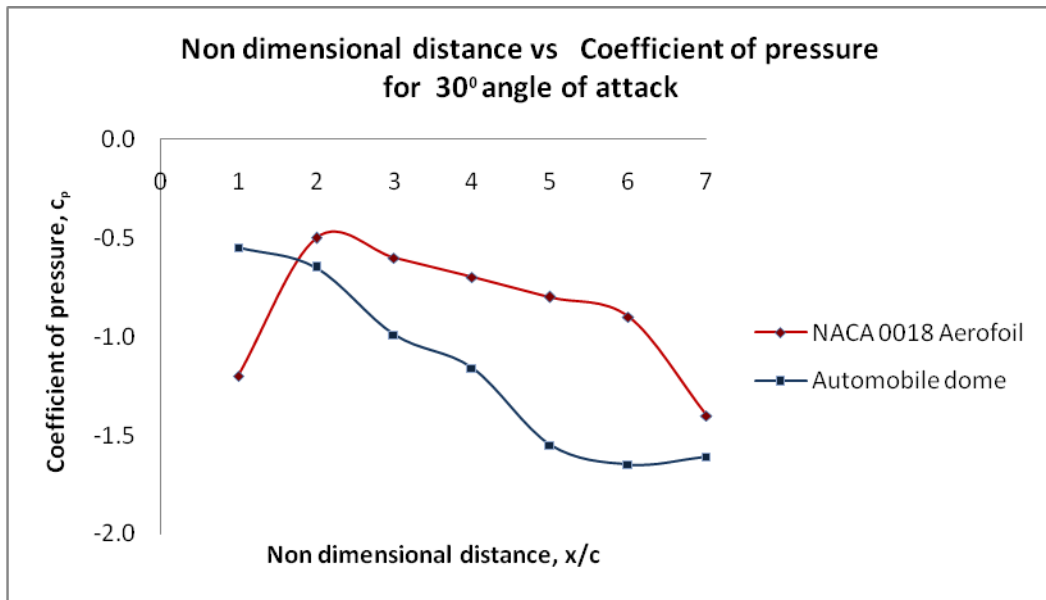


Fig.7

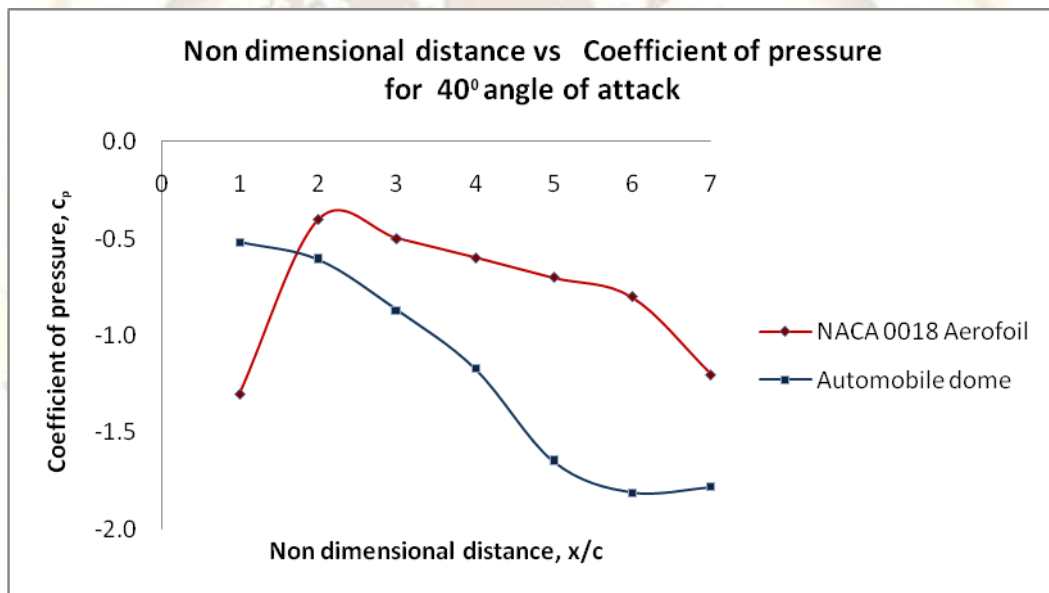


Fig.8

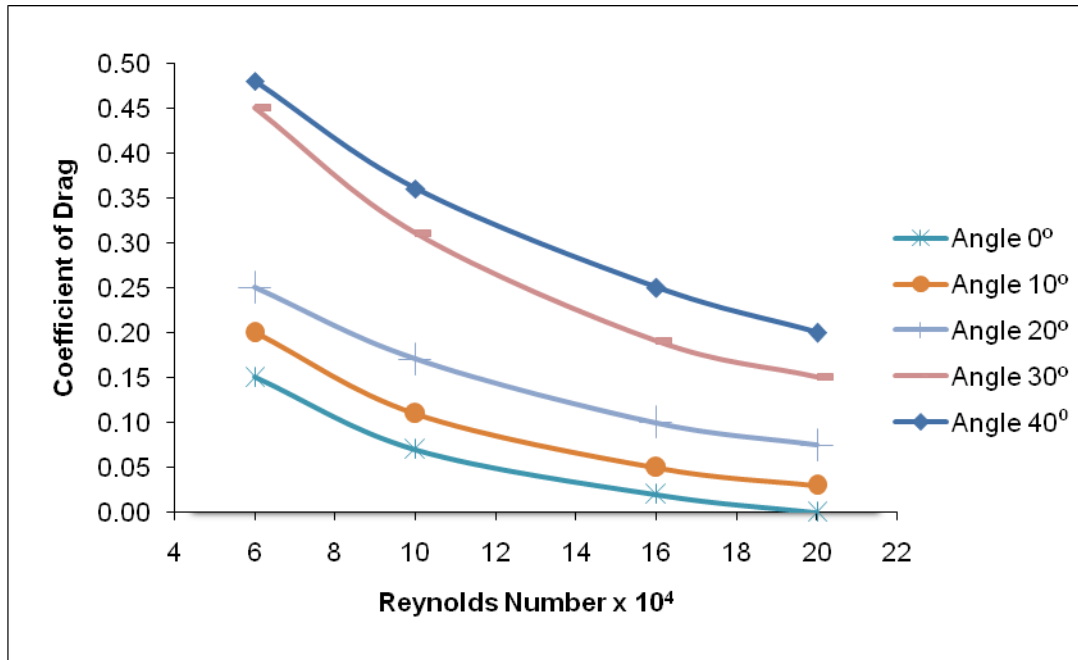


Fig.9

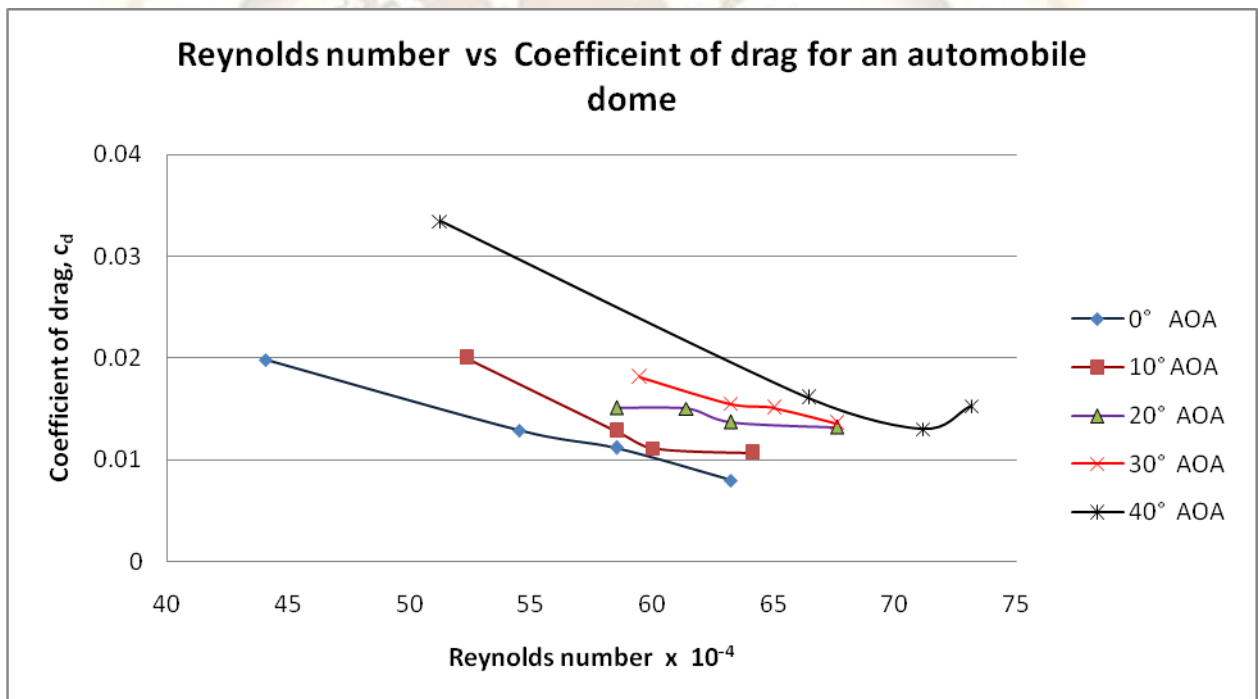


Fig.10